Journal of Engineering Science and Technology
Vol. XX, No. Y (Year) PPP - QQQ

A GRID-CONNECTED HYBRID WIND-SOLAR POWER SYSTEM

MAAMAR TALEB

University of Bahrain
Department of Electrical and Electronics Engineering, P. O. Box 32038, ISA Town – Bahrain
Email: mtaleb@uob.edu.bh

Abstract

A hybrid renewable energy system consisting of a photovoltaic generator and a wind driven DC machine is interconnected with the power utilities grid. The interconnection is done through the use of two separate single phase full wave controlled bridge converters. The bridge converters are operated in the "inverter mode of operation". That is to guaranty the extraction of the real powers from the wind driven generator as well as from the photovoltaic generator and inject them into the power utilities grid. At any pretended surrounding weather conditions, maximum extraction of powers from both renewable energy sources is targeted. This is done through the realization of self-adjusted firing angle controllers responsible of triggering the semiconductor elements of the controlled converters. An active power filter is shunted with the proposed setup to guaranty the sinusoid quality of the power utilities line current. The overall performance of the proposed system has been simulated in MATLAB/SIMULINK environment. Quite satisfactory and encouraging results have been obtained.

Keywords: Renewable energy sources, Integration with grid systems, Wind driven DC machine, Solar energy, Maximum power point tracker, Active power filter.

1. Introduction

It is well known that most (if not all) renewable energy resources suffer from the lack of providing constant power. This is due to the uncontrollable change of the surrounding weather and environmental conditions. A possible and practical solution to overcome the problem of relying on the power generated by the renewable energy resources is to constitute a hybrid DC grid made of a combination of parallel renewable energy resources and storage units and inter-connect it to the AC grid [1-3] or to use three phase bridge inverters [4-5].

Nomenclatures

A, B,C	Parameters whose values depend on the insolation level.
AC	Alternating Current
A_r	area swept by the motor rotor and it is set to $A_r=\pi r^2$
C_p	is a dimensionless performance power coefficient
DC	Direct Current
Ig	Photovoltaic Generator generated Current
p	pitch angle
Pg	Power Generated by the PVG Generator
PVG	Photovoltaic Generator
Po	Power of moving Air
Pw	Mechanical power extracted from the power of moving air
r	radius of the rotor
V_{DC}	Voltage Average Value at the DC side of the Bridge Converters
Vg	Photovoltaic Generator terminals voltage
Voc	open circuit voltage across the terminals of the PVG
V_w	wind speed in meter/second (m/s).

Greek Symbols

α	Firing angle of the thyristors bridge converter
ρ	density of the air which may be taken at normal temperature and pressure as equals to 1.25 kg/m^3
λ	is known as the tip speed ratio.

The DC grid is usually linked to the AC grid through conventional power inverter modules [1-3].

The present paper uses a different power inverter circuit topology. The suggested topology consists of using two single phase full wave controlled bridge converters operating in the "inverter mode of operation". This type of inverters was used by the author in the works reported in references [6-7].

The work done in the present article consists of connecting a separately excited DC machine, driven by a wind turbine, to the power grid through a cascaded setup consisting of one of the single phase full wave controlled converters and a smoothing reactor. Similarly, a photovoltaic generator (PVG) is connected too to the power utilities grid through a cascaded setup consisting of a second single phase full wave controlled converter and a second smoothing reactor. The two previous single phase controlled converters/rectifiers are connected in parallel. To avoid the penetration of the harmonic currents, which are expected to be generated by the controlled converters into the power utilities grid, an active power filter is shunted with the proposed circuit configurations [8]. The operation of the used active power filter is controlled by a hysteresis controller. The duty of the active power filter is guaranty the sinusoid quality of the power utilities line current. To extract the maximum power from the wind driven DC machine as well as from the photovoltaic generator at any surrounding wind speed and insolation levels, maximum power point trackers are added to the

proposed interconnection configurations. The maximum power point trackers perform their task by updating online the firing pulses needed by the semiconductor valves of the two single phase full wave controlled converters. The updated firing angles should be the ones corresponding to the maximum powers that can be extracted from the two renewable energy sources.

The proposed interconnection of the two renewable energy sources with the power utilities grid owns the following merits when compared to its counterpart in the conventional ways of interconnection:

- No need to worry about the synchronization with the AC power utilities grid.
- No need to worry about the level of the generated DC generator voltage. The smoothing reactors allocated at the DC side of the converters take care about any voltage differences.
- No worry about the harmonic currents generated from the proposed configuration. The existence of active power filter will cancel such harmonics and will prevent them from spreading out into the power utilities grid.
- No need to storage units (i.e., batteries).
-

2. Study System

A general scheme of the study system is presented in Fig. 1. The figure consists of four parts: a wind driven DC machine setup operated by a first controlled single phase full wave bridge rectifier, a photovoltaic generator operated by a second controlled single phase full wave bridge rectifier, an AC voltage source representing the power utilities side or the grid, and an active power filter.

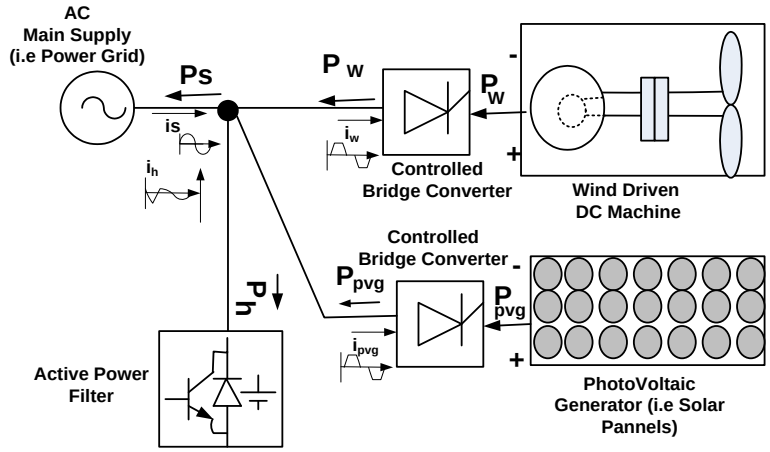

Fig. 1. Study system.

The desired powers flow and the current directions are simplified by the arrows direction. The full wave converters/rectifier as well as the active power filter modules are controlled by external self-tuning controllers. The voltage polarities of the DC machine as well as the one of the photovoltaic generator are reversed in the figure and that is to indicate that the DC machine as well as the

PVG will be generating real powers rather than absorbing real powers. Figure 2 details the contents of Fig. 1.

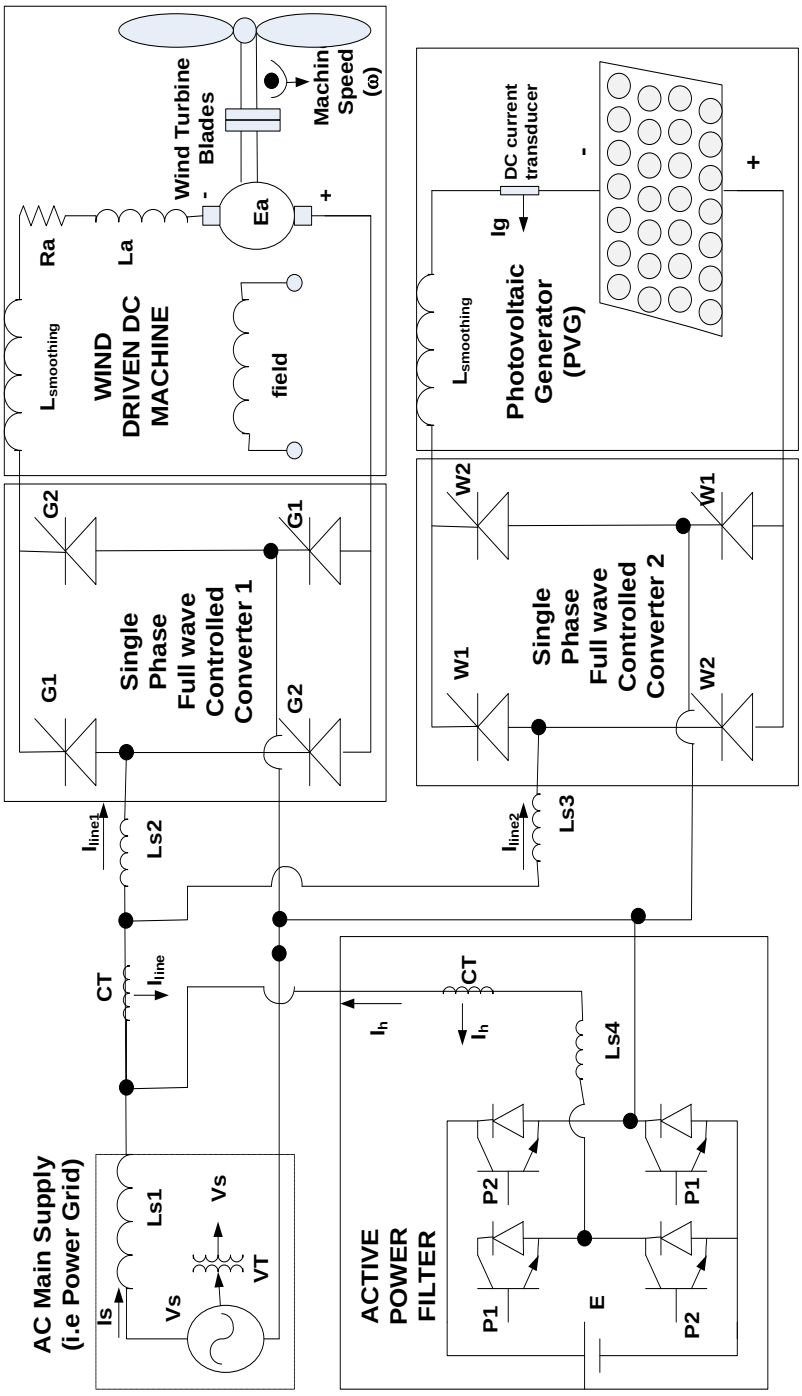

Fig. 2. Detailed circuitry of the study system.

The controllers needed to generate the convenient pulses to trigger the thyristors of the bridge converters as well as the one needed to generate pulses to drive the gates of the IGBT's of the active power filter module are shown in Fig. 3.

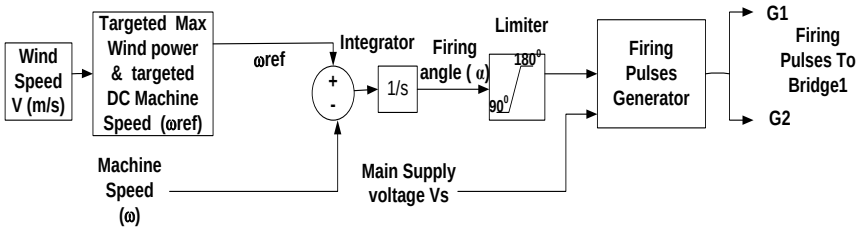

a) Firing angle Controller of the Bridge Converter Carrying the Wind Driven DC Machine

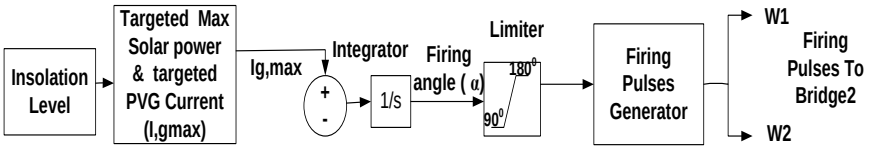

b) Firing angle Controller of the Bridge Converter Carrying the Photovoltaic Generator

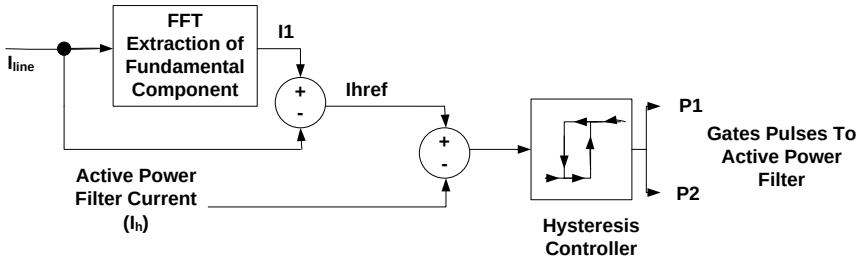

c) Active Power Filter Controller

Fig 3. Controllers of converters of Fig. 2.

The next subsections describe the mathematical model and the operation of the important blocks of Fig. 2.

2.1. Generated wind power

The power of the moving air through a wind rotor can be expressed as [9]:

$$P_o = \frac{1}{2} A_r \rho V_w^3 \quad (1)$$

where $\mathbf{A_r}$ represents the swept area by the motor rotor and it is set to $A_r = \pi r^2$.
r represents the radius of the rotor.
ρ density of the air which may be taken at normal temperature and pressure as equals to 1.25 kg/m^3

$\mathbf{V_w}$ is the wind speed in meter/second (m/s).

The moving air power ($\mathbf{P_o}$) can be converted partially to a mechanical power. The mechanical power that can be extracted from such moving air power can be expressed as [9]:

$$P_w = C_p P_o \tag{2}$$

$\mathbf{C_p}$ is a dimensionless performance power coefficient and its value is naturally always < 1. Investigator of reference [9] proposed a handy formula for Cp in the form of:

$$C_p = C_1(C_2 - C_3 p - C_4 p^x - C_5)e^{-C_6} \tag{3}$$

where C_1= 0.5 , C_2= 116/λ_i, C_3=0.4, C_4=0.1,C_5=5, C_6=21/λ_i, x= 1.5.

$\frac{1}{\lambda_i} = \frac{1}{\lambda + 0.08p} - \frac{0.035}{p^3 + 1}$ and $\lambda = \frac{r\omega_w}{V_w}$

p: pitch angle between the blade element with respect to the plane of rotation.
$\boldsymbol{\lambda}$ is known as the tip speed ratio.

$\mathbf{C_p}$ is maximized when the tip speed ratio $\boldsymbol{\lambda}$ is equal to 7.975340822. The corresponding value of the coefficient C_p at such tip speed ratio is $\mathbf{C_{p,max}}$ = 0.413814988. The previous numbers are found from the derivation done by the author in the appendix of reference [10].

Therefore, the maximum extracted power from the wind turbine is of the form:

$$P_{w,\max} = \frac{1}{2} A_r \rho V_w^3 C_{p,\max} = \frac{0.413814988}{2} A_r \rho V_w^3 \tag{4}$$

Thus, for the sake of extracting maximum wind power ($P_{w,max}$) at a certain wind speed (V_w), the wind driven DC machine speed has to be controlled by the firing angle controller of subfigure Fig. 3(a) and made the DC machine rotating near the following angular reference velocity:

$$\omega_{ref} = \frac{7.975340822 V_w}{r} \tag{5}$$

The firing angle value, in Fig. 3(a), is continuously updated. This is done whenever there is a change in the wind speed which ultimately provides a new reference speed ω_{ref}. The update in the firing angle value is performed through the use of the integrator block. As can be seen from subfigure (i.e., Fig. 3(a)), the input to the integrator block is an error representing the difference between the previous reference speed ω_{ref} and the actual machine speed ω . Thus, when the error reaches of falls within a certain set tolerance band, the output of the integrator settles at a certain value. Such settled value corresponds to a desired firing angle value that secures the maximum extraction of power from the wind turbine prime mover.

The separately excited DC machine is represented by a series combination of the armature resistance (Ra), the armature inductance (La), and the internal generated voltage (Ea). Ea is proportional to the machine speed (ω) and the field flux (ϕ). The field flux is kept constant in this study.

2.2. Photovoltaic generator (PVG) model

The photovoltaic generator Model is of the form [11]:

$$I_g = \frac{(Voc - V_g)}{A + BV_g{}^2 - CV_g} \tag{6}$$

where

Voc: open circuit voltage across the terminals of the PVG generator at an insolation level

A, B, C: are parameters whose values depend on the insolation level.

The PVG model of equation (6) is extended here to represent the PVG by a voltage source model rather than a current source model. Such voltage source model is of the form:

$$V_g = \frac{(CI_g - 1) + \sqrt{(1 - CI_g)^2 + 4BI_g(Voc - AI_g)}}{2BI_g} \tag{7}$$

For a specified insolation level, the voltage V_g times the current I_g determines the power that can be generated from the PVG source.

$$P_g = V_g I_g = \frac{V_g(Voc - V_g)}{A + BV_g{}^2 - CV_g} \tag{8}$$

Under certain pretended insolation level and when $Vg=Vg,max$, the previous power exhibits at maximum power point. Such maximum power point is targeted through the proper operation of the firing angle controller module of Fig 3(b). Such module (i.e., Module of Fig 3(b)) tracks the maximum power point through the enforcement of the photovoltaic generator model current (I_g) to take value near the following current expression:

$$I_{g,\max} = \frac{(Voc - V_{g,\max})}{A + BV_{g,\max}{}^2 - CV_{g,\max}} \tag{9}$$

The expression of Vg,max can be obtained from the analysis done in Appendix A.2 of reference [7].

The firing angle value, in Fig. 3(b), is continuously updated. This is done whenever there is a change in the insolation level which in turns updates the reference PVG current $I_{g,max}$. This update is done through the use of the integrator block. As can be seen from Fig 3(b), the input to the integrator block is an error representing the difference between the previous reference PVG current $I_{g,max}$ and the actual PVG current I_g . Thus, when the error reaches of falls within a certain set tolerance band, the output of the integrator settles at a certain value. Such settled value corresponds to a desired firing angle value that secures the maximum extraction of power from the photovoltaic generator.

2.3. Controlled converters

The controlled converters are no more than controlled single phase full wave bridge rectifiers. Each rectifier is operated in a mode termed "Inverter Mode of Operation". In a such mode of operation, the firing angle provided to the SCRs valves of the bridge should be greater than 900. The average value of the voltage at the dc side of the bridge rectifiers will be obeying the following expression:

$$V_{DC} = K_1 \cos(\alpha) \tag{10}$$

where K1 is a positive constant and it is proportional to the RMS value of the main AC supply voltage and α represents the firing angle.

For any value of the firing angle greater than 900, the average voltage VDC is negative. A negative value of the voltage VDC times a positive value of the current that circulates in the smoothing reactor, located at the DC side of the converter, results in a negative value for the power at the DC side of the controlled converter/bridge rectifier. That leads to the statement that such power is generated by the renewable energy source (either the wind driven DC machine or the photovoltaic generator) and it is injected into the AC side of the Converter.

2.4 Active power filter

The use of the controlled single phase full wave bridge converters/rectifiers alone results in the distortion of the line current (Iline). The distortion of the line current will generate harmonic currents. Such harmonic currents penetrate into the power grid and causes undesirable effects. Therefore, it is necessary that a shunt filter should be allocated at the point of interconnection found between the power utilities grid and the controlled converter. The active power filter proposed in reference [8] is one of the solutions to the problem of undesired generated harmonic currents. The used active power filter is voltage source inverter, as shown in the left bottom side of Fig. 2. The active power filter performs its tasks as follows:

- a reference signal (Ihref) is generated or calculated online. It consists of the difference between the fundamental component of line current (Iline) entering the bridge rectifiers and the line current (Iline) itself.
- a measured current (Ih) located at the AC side of the bridge inverter is subtracted from the previous reference signal (Ihref).

- the result of the previous subtraction is fed to a hysteresis controller. The output of the hysteresis controller is high or low and it is passed to the gates of the IGBTs having the attributions (P1) in Fig. 2. The signal passed to the gates of the IGBTs having the attributions (P2) in Fig. 2 is the just the complementary of the output signal (P1) obtained from the hysteresis controller.
- under steady state conditions, the current (Ih) at the AC side of the bridge inverter is nearly equal to:

$$I_h = i_1 - I_{line} = I_{href} \tag{11}$$

where $\mathbf{i_1}$ is the fundamental component of the line current ($\mathbf{I_{line}}$) the summation of the currents entering both converters of Fig. 2 from the AC side.

Applying Kirchhoff's current law, at the point of the connection of the active power filter, results that the current drawn from the power utilities grid

$$I_s = I_{line} + I_h = I_{line} + i_1 - I_{line} = i_1 \tag{12}$$

Thus, the supply current **Is** will be free from harmonic currents/components.

The operation of the IGBTs of the active power filter is activated by the pulses generated by the controller of Fig. 3(c). The pulses are generated by a hysteresis controller that is in turns controlled online by the difference between a reference harmonic current (Ihref) and a current (Ih), measured at the AC side of the active power filter.

3. System Performance

The performance of the proposed interconnection of Fig. 2 has been evaluated using computer simulations. MATLAB/SIMULINK has been used in the computer simulations. The system data used in the simulations are provided in Table 1.

Table 1. System data.

DC machine			
Armature resistance Ra= 0.4832 Ω	**Armature inductance La= 6.763 mH**	**Field resistance Rf=220 Ω**	**Field inductance Lf=110 H**
Field Voltage Vf=220 V	**Moment of Inertia J=0.2053 kg.m^2**	**Field-Armature Mutual Inductance Laf=Kϕ= 1 H**	**DC smoothing Coil Inductances 0.5 H**
Wind turbine			
Blades length (r) = 120 cm			
Photovoltaic generator (PVG)			
Insolation Level (%)	**Voc (V)**	**A (Ω)**	**B (1/AV) *10^3**	**C (1/A)**
100	**176**	**12.94**	**0.119**	**0.0819**
90	**174**	**13.96**	**0.129**	**0.089**
80	**170.5**	**15.81**	**0.165**	**0.1047**

70	**167**	**17.95**	**0.182**	**0.1198**
60	**164**	**20.01**	**0.209**	**0.1359**
50	**160.5**	**22.70**	**0.247**	**0.1573**
40	**153**	**29.71**	**0.2386**	**0.2022**

AC main supply			
Rms Voltage 240 V	**Frequency 50 Hz**	**Phase angle 0^0**	**Leakage inductances Ls1 =Ls2=Ls3= 2.5 mH,**

Active power filter		
DC Voltage source E=400 V	**Leakage inductance Ls4 =5 mH**	**Hysteresis controller Current Band 0.04 A**

For certain pretended wind speed and insolation levels, the performance looked for consists of:

- recording continuously the maximum power that can be extracted from the wind turbine, the input power delivered by the DC machine, and the power delivered by the DC machine to the AC side of the bridge rectifier number 1,
- - recording continuously the maximum power that can be extracted from the photovoltaic generator (PVG), and the power delivered by the PVG to the AC side of the bridge rectifier number 2,
- - recording continuously the power absorbed by the active power filter,
- - recording continuously the net power delivered to the power utilities grid,
- - recording continuously the reference and the actual/measured speeds of the DC machine,
- - recording continuously the firing angles updated values,
- - calculating continuously the total harmonic distortion factor (**THD**) in the supply current
- - calculating continuously the displacement power factor at the supply side bus,
- - recording continuously the time-varying waveforms of: the main AC supply voltage, the supply current, the current entering the bridge converters, the total currents drawn by the two controlled converters, the current supplied by the active power filter and the reference/desired current of the active power filter.

Three surrounding weather conditions cases were pretended and simulated.

Figure 4 depicts the steady state quality of power utilities bus voltage, the power utilities line current, the current drawn by bridge converter #1, the current drawn by bridge converter #2, the sum of the previous two currents, and the active power filter current and its desired/reference waveforms.

The first column waveforms in Fig. 4 are obtained under pretending 3 m/s wind speed and 100% insolation levels. The second column waveforms are obtained under pretending 4 m/s wind speed and 70% insolation levels. The third column waveforms are obtained under pretending 5 m/s wind speed and 50% insolation levels.

Examining the waveforms of the power utilities line current, shown in Fig. 4, under the pretended weather conditions cases, indicates that a very minor distortion is encountered in such power utilities line current. This means the

active power filter has performed its task adequately. Table 2 reports their steady state numerical values of the powers delivered or absorbed by the different modules of Fig. 2. Such power values are also depicted in the charts of Fig. 5. The simulink file to duplicate the results of either Fig. 4 or table 2 can be obtained by contacting the author at his email: mtaleb@uob.edu.bh.

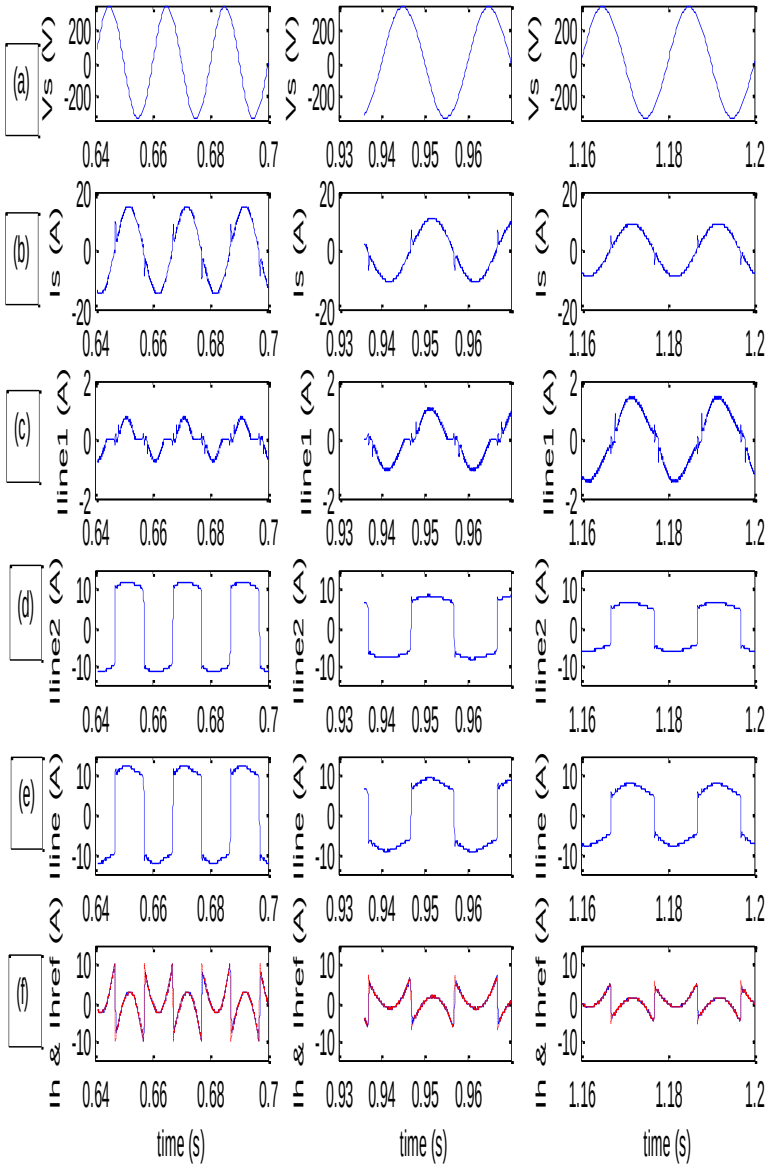

Fig. 4. Simulation results: a) Supply voltage b) Power Utilities Current (Supply current) c) Current Drawn by the Bridge Converter carrying the Wind Driven DC Machine, d) Current Drawn by the Bridge Converter carrying the Photovoltaic Generator, e) Summation of the currents of parts c) and d), f) active power filter current and its desired reference waveform.

Table 2. Study system results.

	Case 1 Insolation level = 100% Wind speed = 3m/s	Case 2 Insolation level = 70% Wind speed = 4m/s	Case 3 Insolation level = 50% Wind speed = 5m/s
Maximum power that can be extracted from the wind turbine Pw,max (W)	**31.5909**	**74.8822**	**146.25**
Input Power to the DC Machine (W)	**29.2864**	**68.3280**	**145.5442**
Power delivered by the DC machine at the AC side of the bridge converter1 Pw (W)	**28.1231**	**66.4350**	**141.2861**
Firing angle Of the bridge converter 1 α (0)	**146.5**	**141**	**139.5**
Maximum power that can be extracted from the PVG Ppvg,max (W)	**1399**	**910.9052**	**664.4722**
Power delivered by the DC machine at the AC side of the bridge Converter2 Ppvg (W)	**1390**	**902.4663**	**659.0224**
Firing angle Of the bridge converter2 α (0)	**123**	**122**	**121.5**
Power absorbed By the active power filter Ph (W)	**46.7148**	**30.6709**	**18.5136**
Net Power Delivered to the AC power Utilities Grid Ps (W)	**1346.8**	**932.3353**	**788.0803**
Displacement Power Factor at the power Utilities Bus	**-0.5269**	**-0.5017**	**-0.5098**
Total Harmonic Distortion Factor in the power utilities line current THD (%)	**10.7528**	**9.3763**	**7.8117**

A glance at the second, third, and fourth columns of Table 2, one can clearly notice that nearly maximum power are extracted from the wind turbine as well as from the PVG generator at the pretended wind speed and insolation levels. Thus, it can be said the firing angle controllers of Fig. 3 are performing the role of the maximum power point trackers.

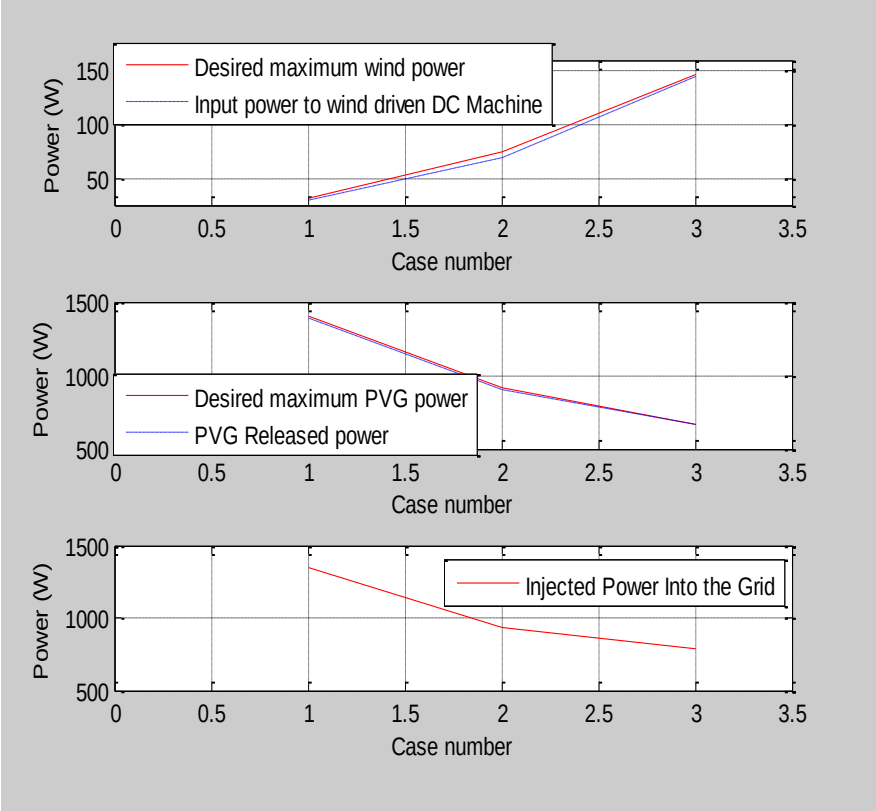

Fig. 5. Simulation results: Upper graph represents the anticipated maximum wind power and the input power to the wind driven DC machine. Middle graph represents the anticipated maximum PVG power, the power obtained from the PVG. Lower graph represents the overall power injected into the grid for cases:

Case1: Insolation level = 100%, Wind speed = 3m/s, **Case2:** Insolation level = 70%, Wind speed = 5m/s, **Case3:** Insolation level = 50%, Wind speed = 5 m/s.

4. Conclusion

Interconnecting a hybrid renewable energy system consisting of a wind driven DC machine and a photovoltaic generator (PVG) with a power utilities grid has been investigated in this paper. The interconnection has been done through the installation of controlled single full wave bridge rectifier/converters. A shunt active power filter has been installed between the AC supply and the converter and that is to get rid of the undesired harmonic currents

The performance of the overall installation has been tested through computer simulations. Maximum powers are nearly extracted from the wind driven DC machine as well as from the photovoltaic generator under certain pretended weather conditions (as depicted in Fig. 5). A nearly pure sinusoid waveform has been observed in the AC grid current under the pretended weather conditions (as depicted in Fig. 4(b)).

References

1. Chedid, R.; Akiki, H.; and Rahman, S. (1998), A decision support technique for the design of hybrid solar-wind power systems. *IEEE Transactions on Energy Conversio*n, 13(1), 76-83.
2. Biczel P. and Koniak M. (2009), Design of power plant capacity in DC hybrid system and microgrid. *Proceedings of the Fourth International Conference On Ecological Vehicles and Renewable Energies (EVER09*), Monte Carlo, Monaco.
3. IEEE Standard for Interconnecting Distributed Resources with Electric Power Systems. (2003), *Standard IEEE 1547-2003*.
4. Rajashekar A. ,Swathi S. , Sadanandam P. , and Yasin Md. (2013), Grid Interconnection of Renewable Energy Sources with Power-Quality Improvement Features at the Distribution Level, *International Journal of Engineering Research and Applications (IJERA)*, 3 (3), 741-745.
5. Singh M., Khadkikar V. , Chandra A., and Varma R. (2011), Grid Interconnection of Renewable Energy Sources at the Distribution Level With Power-Quality Improvement Features, *IEEE Trans. on Power Delivery*, 26 (1), 307-315
6. Taleb M. , Salman H., Jumaa H. and Al-Mukharreq H. (2012), Performance of a Hybrid Wind-Grid-Load Energy System, *Journal of Technology Innovations in Renewable Energy*, 1 (1), 48-52.
7. Taleb M. (2011). Interconnection of a photovoltaic generator (PVG) to a main supply: A simulation study. *Renewable Energy and Power Quality Journal*, 9(1).
8. Rahmani S., Al-Haddad K., Kanaan H. Y. (2006), A comparative study of shunt hybrid and shunt active power filters for single-phase applications: Simulation and experimental validation, *Mathematics and Computers in Simulation*, 71 (4–6), 345-359.
9. Heier S. (1998), *Grid Integration of Wind Energy Conversion Systems*, John Wiley & Sons Company.
10. M. Taleb M. (2004), Optimal Operation of a Wind Driven System. *Journal of King Saud University, {Engineering Sciences}*, 16(2), 229-252.
11. Akbaba M. (2003), Matching of AC loads to PVG for Maximum Power Transfer Using an Enhanced Version of Akbaba Model and Double Step-up Converter, *International Journal of Solar Energy*, 75 (1), 17-25.